Radiolabeled Peptides for Targeting Cholecystokinin-B/Gastrin Receptor-Expressing Tumors

Thomas M. Behr, Niels Jenner, Martin Béhé, Christa Angerstein, Stefan Gratz, Friedhelm Raue and Wolfgang Becker

Department of Nuclear Medicine, Georg-August-University, Göttingen, Germany; and Department of Endocrinology, Ruprecht-Karl-University, Heidelberg, Germany

The high sensitivity of pentagastrin stimulation in detecting primary or metastatic medullary thyroid cancer (MTC) suggests widespread expression of the corresponding receptor type on human MTC. Indeed, autoradiographic studies have demonstrated cholecystokinin (CCK)-B/gastrin receptors not only in more than 90% of MTCs but also in a high percentage of small cell lung cancers, some ovarian cancers, astrocytomas and potentially a variety of adenocarcinomas. The aim of this study was to systematically screen and optimize, in a preclinical model and a pilot clinical study, suitable radioligands for targeting CCK-B receptors in vivo. **Methods:** A variety of CCK/gastrin-related peptides, all bearing the C-terminal CCK receptor-binding tetrapeptide sequence Trp-Met-Asp-PheNH$_2$ or derivatives thereof, were studied. They were radioiodinated by the Iodogen or Bolton-Hunter procedures. The peptides were members of the gastrin or CCK families, which differ by the intramolecular position of a tyrosyl moiety. Their stability and affinity were studied in vitro and in vivo; their biodistribution and therapeutic efficacy were tested in nude mice bearing subcutaneous human MTC xenografts. Diethylenetriamine pentaacetic acid (DTPA) derivatives of suitable peptides were synthesized successfully, and their preclinical and initial clinical evaluations were performed, labeled with ^{111}In. **Results:** All members of the CCK or gastrin families were stable in serum (with half-lives of several hours at 37°C); nevertheless, the stability of those peptides bearing N-terminal pGlu residues or D-amino acids was significantly higher. In accordance with their comparably low affinity, nonsulfated members of the CCK family showed fairly low uptake in the tumor and other CCK-B receptor-expressing tissues. Sulfated CCK derivatives performed significantly better but also displayed a comparably high uptake in normal CCK-A receptor-expressing tissues. This effect was probably due to their similar affinity for both CCK-A and CCK-B receptors. Best tumor uptake and tumor-to-nontumor ratios were obtained with members of the gastrin family because of their selectivity and affinity for the CCK-B receptor subtype. Pilot therapy experiments in MTC-bearing animals showed significant antitumor efficacy compared with untreated controls. DTPA derivatives of minigastrin were successfully developed. In a pilot clinical study, radioiodinated and ^{111}In-labeled derivatives showed excellent targeting of physiological CCK-B receptor-expressing organs, as well as all known tumor sites. **Conclusion:** CCK/gastrin analogs may be a useful new class of receptor-binding peptides for diagnosis and therapy of CCK-B receptor-expressing tumors, such as MTC or small cell lung cancer. Nonsulfated gastrin derivatives may be preferable because of their CCK-B receptor selectivity, hence lower accretion in normal CCK-A receptor-expressing organs.

Key Words: gastrin; cholecystokinin; cholecystokinin-B/gastrin receptors; radiolabeled peptides; medullary thyroid cancer; small cell lung cancer

T he development of regulatory peptides as tools to visualize and, more recently, to treat malignant tumors has been an important focus of interest over the past years (1–3). The successful development of sufficiently stable radiolabeled somatostatin analogs, such as ^{123}I-Tyr^3- or ^{111}In diethylenetriamine pentaacetic acid (DTPA)-D-Phe^1-octreotide, for diagnostic puposes (1,2) and the introduction of ^{161}Tb-DTPA or ^{90}Y-DOTA conjugates for therapeutic applications have opened new horizons in nuclear oncology (3–5). Other regulatory peptides, such as vasoactive intestinal polypeptide (6), substance P (7) and gastrin-releasing peptide/bombesin derivatives (8), have emerged as potentially useful candidates for in vivo scintigraphy and radiopeptide therapy.

Although somatostatin receptor scintigraphy has proven to be a valuable tool for staging gastroenteropancreatic tumors (e.g., carcinoids), its sensitivity and accuracy in other neoplasms, such as medullary thyroid cancer (MTC) and small cell lung cancer, are limited (9–11). Because of the outstanding diagnostic accuracy of the pentagastrin test in detecting the presence, persistence or recurrence of malignant C cells (even when they are smaller than a size detectable by conventional morphological imaging methods), we postulated the expression of the corresponding receptor type in human MTC (12). Indeed, receptor autoradiographic studies have demonstrated the expression and presence of cholecystokinin (CCK)-B/gastrin receptors not only in more than 90% of MTCs (13) but also in a high percentage of other tumor types, such as small cell lung cancer, stromal ovarian cancers and astrocytomas (14).

Previous studies suggested an even more widespread occurrence of gastrin receptors in colon, pancreatic and stomach cancers (15). Therefore, we undertook pilot experiments in nude mice bearing human MTC xenografts and were able to demonstrate the feasibility of radiolabeled gastrin-I to target CCK-B receptor-expressing tumors, as well as CCK receptor-expressing normal organs such as the stomach, in vivo in animals and patients (12).

However, a variety of problems remained to be solved, such as the molecular characteristics that render the peptide an optimal candidate for in vivo targeting of CCK-B receptor-expressing tumors, considering in vivo stability;

affinity to and selectivity for the CCK-B receptor; or the potentially unfavorable accretion in normal organs, such as the liver, bowel, or kidney. The aim of this study, therefore, was to develop and optimize, in a preclinical model as well as in a pilot clinical study, suitable radioligands for targeting CCK receptors in vivo.

MATERIALS AND METHODS

Peptides and Radioiodination

We investigated various peptides in this study (Table 1). They either belong to the gastrin or CCK superfamilies or possess characteristics of both (16). Both families differ by the location of

TABLE 1
Structures and Estimates of the IC_{50} Values of the Radiolabeled Peptides Tested

Peptide	Chain length	Amino acid sequence	Label	IC_{50}
Gastrin derivatives				
Big-gastrin	34	pGlu-Leu-Gly-Pro-Gln-Gly-Pro-Pro-His-Leu-Val-Ala-Asp-Pro-Ser-Lys*-Lys*-Gln-Gly-Pro-Trp-Leu-Glu-Glu-Glu-Glu-Glu-Ala-Tyr†-Gly-**Trp-Met-Asp-PheNH₂**	I, BH	$\sim 0.5 \times 10^{-8}M$
Gastrin-I	17	pGlu-Gly-Pro-Trp-Leu-Glu-Glu-Glu-Glu-Glu-Ala-Tyr†-Gly-**Trp-Met-Asp-PheNH₂**	I	$\sim 10^{-9}M$
[Leu¹⁵]-gastrin-I	17	pGlu-Gly-Pro-Trp-Leu-Glu-Glu-Glu-Glu-Glu-Ala-Tyr†-Gly-**Trp-Leu-Asp-PheNH₂**	I	$\sim 10^{-9}M$
[Gln₅⁶⁻¹⁰]-gastrin-I	17	pGlu-Gly-Pro-Trp-Leu-Gln-Gln-Gln-Gln-Ala-Tyr†-Gly-**Trp-Met-Asp-PheNH₂**	I	$\sim 10^{-8}M$
Minigastrin	13	*Leu-Glu-Glu-Glu-Glu-Glu-Ala-Tyr†-Gly-**Trp-Met-Asp-PheNH₂**	I, BH	$\sim 10^{-9}M$
[D-Leu¹]-minigastrin	13	*D-Leu-Glu-Glu-Glu-Glu-Glu-Ala-Tyr†-Gly-**Trp-Met-Asp-PheNH₂**	I	$\sim 10^{-9}M$
[Gln₅²⁻⁶]-minigastrin	13	Leu-Gln-Gln-Gln-Gln-Ala-Tyr†-Gly-**Trp-Met-Asp-PheNH₂**	I	$\sim 10^{-8}M$
Gastrin-I fragment 11–17	7	Ala-Tyr†-Gly-**Trp-Met-Asp-PheNH₂**	I	$\sim 10^{-8}M$
Gastrin-I fragment 1–14	14	pGlu-Gly-Pro-Trp-Leu-Glu-Glu-Glu-Glu-Ala-Tyr†-Gly-Trp	I	$> 10^{-4}M$
Cholecystokinin (CCK) derivatives				
Caerulein	10	pGlu-Gln-Asp-Tyr†-Thr-Gly-**Trp-Met-Asp-PheNH₂** SO₃⁻	I	$\sim 10^{-8}M$
[Thr²⁸, Nle³¹]-sCCK-25-33	9	*Arg-Asp-Tyr-Thr-Gly-**Trp-Nle-Asp-PheNH₂** SO₃⁻	BH	$\sim 0.5 \times 10^{-9}M$
sCCK-8	8	*Asp-Tyr-Met-Gly-**Trp-Met-Asp-PheNH₂**	BH	$\sim 0.5 \times 10^{-9}M$
nsCCK-8	8	*Asp-Tyr†-Met-Gly-**Trp-Met-Asp-PheNH₂** SO₃⁻	I, BH	$\sim 10^{-8}M$
[Tyr(SO₃H)²⁷] CCK 26–29	4	*Asp-Tyr-Met-GlyNH₂	BH	$> 10^{-4}M$
Peptides with common features of both gastrin and CCK				
Cionin	8	SO₃⁻SO₃⁻ *Asn-Tyr-Tyr-Gly-**Trp-Met-Asp-PheNH₂**	BH	$\sim 0.5 \times 10^{-9}M$
des-BOC-pentagastrin	5	*β-Ala-**Trp-Met-Asp-PheNH₂**	BH	$\sim 0.5 \times 10^{-7}M$
CCK fragment 30–33 (CCK-4)	4	*Trp-Met-Asp-PheNH₂	BH	$\sim 10^{-7}M$
Radiometal-chelate derivative				
DTPA-minigastrin or its [D-Leu¹] analog	13	DTPA-Leu-Glu-Glu-Glu-Glu-Glu-Ala-Tyr-Gly-**Trp-Met-Asp-PheNH₂**	¹¹¹In³⁺	$\sim 10^{-9}M$

*The potential attachment sites of the radioiodinated Bolton-Hunter moieties.
†Tyrosyl moieties that may be radioiodinated by the Iodogen procedure.
I = Iodogen; BH = Bolton-Hunter radioiodination.
Amino acid sequences in boldface indicate the receptor binding sequence.

their tyrosyl moiety, with one amino acid in the gastrin family (usually Gly) or two amino acids in the CCK family (Met-Gly or Thr-Gly) between this very tyrosine moiety and the C-terminal receptor-binding sequence Trp-Met-Asp-PheNH$_2$. Cionin can be phylogenetically regarded as an ancestor of both CCK and gastrin because it bears two tyrosyl residues (one in each position). Finally, the structures of des-BOC-pentagastrin and CCK fragment 30–33 (CCK-4) are basically confined to the receptor-binding sequence common to both the gastrin and CCK families. Two peptides, lacking this (complete) receptor-binding tetrapeptide, served as irrelevant controls: gastrin-I fragment 1–14 and [Tyr(SO$_3$H)^{27}] CCK 26–29 (Table 1).

The peptides were commercially obtained (Sigma Chemie, Deisenhofen, Germany; ICN Biomedicals, Eschwege, Germany; or Bachem Biochemicals, Heidelberg, Germany), whereas [Gln$_5$$^{6-10}$]-gastrin-I, [Gln$_5$$^{2-6}$]-minigastrin, D-Leu^1-minigastrin and gastrin-I fragment 11–17 were synthesized by Genosys Biotechnologies (Cambridge, England). The peptides were stored frozen as lyophilized powder at −20°C. Immediately before use, the peptides were dissolved in 0.05-mol/L aqueous NH$_4$OH at concentrations between 1 and 10 mg/mL.

^{131}I and ^{125}I were purchased as sodium iodide in 0.1-mol/L NaOH (New England Nuclear DuPont, Brussels, Belgium). Radio-iodination by the Iodogen method was performed, as described previously (12), at a specific activity of up to 7.4–9.3 GBq (200–250 mCi) per milligram of peptide (corresponding to molar ratios of radioiodine to peptide between 0.2 and 1.0). Purification from unreacted iodine was performed by gel filtration chromatography (12). Radiochemical purity was shown by high-performance liquid chromatography (HPLC) (Nucleosil 120–3 ^{18}C, 250 × 4 mm, Marchery-Nagel; solvent A: 0.1% trifluoroacetic acid (TFA) in water; solvent B: AcCN; flow rate 0.5 mL/min; gradient: 0–5 min 100% solvent A, 0% solvent B; 5–15 min 20% solvent A, 80% solvent B).

Radioiodination by the Bolton-Hunter procedure was performed with slight modifications from the original procedure (17). Briefly, 2.5 mg of crystalline succinimidyl-3-(4-hydroxyphenyl-)propionate (Sigma Chemie) were dissolved in 10 mL of 0.25-mol/L phosphate-buffered saline (PBS), pH 7.5. One hundred microliters of this solution were mixed with 370 MBq (10 mCi) radioiodine (Na^{131}I or Na^{125}I) in 400 µL of 0.25-mol/L PBS, pH 7.5, and 2 mg of chloramine-T (Sigma Chemie). The reaction was stopped after 10 s by the addition of 1.2 mg sodium metabisulfite in 600 µL of 0.05-mol/L PBS, pH 7.5. After the addition of 200 µL dimethylformamide, the radioiodinated Bolton-Hunter reagent was extracted with two 500-µL portions of benzene and recovered by evaporating the solvent under a gentle stream of dry nitrogen. The peptide (100 µg) was added in 200 µL of 0.1-mol/L sodium borate, pH 8.5, in an ice bath. After vortexing the mixture for 15 min in the ice bath, the reaction mixture was separated on a Sephadex G-25 Superfine column (1 × 55 cm). The radiochemical purity was shown by HPLC, as described above.

Synthesis of DTPA Derivatives and Labeling with ^{111}In

Five milligrams of minigastrin (Bachem Biochemicals) or its [D-Leu^1]-derivative (Genosys) were dissolved in 1 mL of 0.05 mol/L aqueous NH$_4$OH. Two hundred microliters of 2-mol/L NaHCO$_3$ were added, and the pH was adjusted to 8 with 1-mol/L HCl. Cyclic DTPA anhydride (Sigma Chemie) was added as a dry powder (18) in 10-fold molar excess over the peptide (i.e., 12 mg). After incubating the reaction mixture for 60 min at room temperature, it was diluted to 10 mL with water. This solution was applied

to a DEAE Sephadex A-50 weakly basic anion exchange resin column (dimensions: 1 × 20 cm) at 4°C, pre-equilibrated with 10 bed volumes each of saturated 2- and 0.05-mol/L NH$_4$HCO$_3$. The column was eluted at 4°C with 30 mL of 0.05-mol/L NH$_4$HCO$_3$, followed by a linear gradient of 0.05- versus 2-mol/L NH$_4$HCO$_3$ (150 mL each) (19). The elution of the peptide was monitored by determination of the absorbance at 280 nm and by a modified bicinchoninic acid procedure (Micro BCA® Assay; Pierce, Rockford, IL). Fractions containing the DTPA-derivatized peptide were combined and lyophilized. The peptide was stored frozen at −20°C in 0.5-mol/L NH$_4$OAc/0.05-mol/L ammonium ascorbate at a pH of 5.5 in a concentration of 5 mg/mL. Immediately before use, the peptide was thawed. ^{111}In chloride (Mallinckrodt, Petten, The Netherlands) was added in 100 µL of 0.5-mol/L NH$_4$OAc, pH 5.5, to yield a specific acitivity of up to 15 MBq (400 µCi) per microgram of peptide. The radiochemical purity was shown by HPLC, as described above.

Serum Stability Testing In Vitro

For the assessment of the serum stability of the various radiolabeled peptides in vitro, the radiolabeled peptides (typically 7.4 MBq [200 µCi], 1 µg) were added to 2 mL serum from a healthy donor at 2°C. Conventional low-pressure gel filtration chromatography (on a Sephacryl S-300-HR [Sigma Chemie] column; dimensions: 1 × 100 cm) and/or size-exclusion HPLC (Bio-Sil SEC-250 column; dimensions: 300 × 7.8 mm; Bio-Rad Laboratories, Richmond, CA) was performed immediately after the serum addition or after incubation periods of 1, 4 and 24 h at 2°C and of 1, 4 and 24 h at 37°C (20).

For redox experiments, the labeled peptides were incubated for 1 h at 37°C in 1-mol/L H$_2$O$_2$ or for 48 h in 1-mol/L dithiothreitol (21). Subsequent HPLC analysis was performed as described above (Nucleosil 120–3 ^{18}C, 250 × 4 mm, Marchery-Nagel).

Affinity/IC$_{50}$ Determination

The 50% inhibitory concentrations (IC$_{50}$ values) of the various radiolabeled peptides were determined in cell suspension. Briefly, single cell suspensions of TT cells (22) (for details, see below) in Ham's F12K medium (ICN Biomedicals), supplemented with 0.1% NaN$_3$, were incubated for 1 h in polyethylene cups at room temperature with ^{125}I-gastrin-I in a concentration of 50 pmol/L and various increasing concentrations of the respective nonradioactive peptides to generate competitive inhibition curves. Sodium azide was added to avoid any removal of receptor-bound radioligands from the equilibrium by means of internalization. After 1 h, the samples were spun down, and the pellets were washed three times with ice-cold Ham's F12K medium (0.1% NaN$_3$) and counted in the scintillation counter. The data were plotted as peptide concentrations versus specific binding, and IC$_{50}$ values were derived.

Human Medullary Thyroid Cancer Model in Nude Mice

The human MTC cell line, TT (American Type Culture Collection, Rockville, MD), was cultured at 37°C in Ham's F12K medium and supplemented with 10% fetal-calf serum (Sigma Chemie), as described previously in more detail (22,23). TT is a heterozygous carrier of a mutation in codon 634 of exon 11 of the RET proto-oncogene (TGC → TGG, corresponding to the amino acid exchange Cys → Trp) (23).

Approximately 10^7–10^8 cells were inoculated subcutaneously into female nude mice, 19–23 g and 4–5 wk old (Charles River, Sulzfeld, Germany). Subsequently, the tumors were serially propagated by preparing a mince through a 40-mesh screen and rinsing

with Ham's F12K medium, supplemented with 20% fetal-calf serum, to yield a 20% cell suspension. Two hundred fifty microliters of this suspension were injected subcutaneously. After approximately 3–4 wk, tumors approximately 100–200 mg in size (the size used in this study) had developed in more than 90% of the animals.

Biodistribution Studies

Tumor-bearing animals were injected intravenously into the tail with the [131]I-, [125]I- or ^{111}In-labeled peptide (740–1480 kBq [20–40 μCi], 0.5–1.0 μg). The mice were killed at 10 min or 1, 3, 5 or 24 h. They were bled by retro-orbital puncture, and, after cervical dislocation, the animals were dissected. For determination of the whole-body retention, whole mice were measured in a well counter. The amount of activity in the tumor and tissues (lung, liver, spleen, kidney, stomach, pancreas, gallbladder, intestine, brain, adrenals, muscle, bone and blood) was determined by gamma scintillation counting using an injection standard to account for physical decay (23,24). The number of animals used for each study was typically 5 per group at each time point. In several studies, animals were coinjected with a mixture of [131]I- and ^{125}I-labeled peptides. In these instances, windows were set for each radionuclide, and the backscatter of ^{131}I into the ^{125}I window was corrected. To assess specificity of receptor binding, parallel groups of mice were given either 1 μg of radiolabeled peptide alone or 1 μg of radiolabeled peptide supplemented with 1 mg of unlabeled peptide.

Experimental Radiopeptide Therapy

Tumor sizes were determined by caliper measurement in three dimensions immediately before therapy and at weekly intervals thereafter. Tumor volumes were estimated by multiplying the product of the three perpendicular diameters by 0.5, assuming an elliptical geometry (23). Tumors were left untreated (controls), given unlabeled gastrin-I or injected with a single dose of ^{131}I-labeled gastrin-I or gastrin-I fragment 1–14. Ten to 20 animals were studied in each group. Body weight was recorded weekly, and survival was monitored (23,24). The maximum tolerated dose was defined as the highest possible activity under the respective conditions that did not result in any animal deaths, with the next 10%–20% higher dose level resulting in at least 10% of the animals dying (23,24). Total and differential white blood cell and platelet counts were determined on the day of therapy and at weekly intervals thereafter. Seventy-five-microliter heparinized specimens were collected by retro-orbital bleeding. The samples were counted on a Technicon H3 Auto-Analyzer (Bayer-Diagnostik, Munich, Germany). Blood urea nitrogen and creatinine as indicators of renal function, as well as glutamate oxaloactetate transaminase and alkaline phosphatase as liver function parameters, were determined at the same time points as the blood counts. Means ± SDs were calculated for each group (23,24).

Initial Clinical Evaluation of ^{131}I-Labeled Gastrin-I and ^{111}In-DTPA-Minigastrin

After premedication with omeprazole (20 mg orally, given 2 h before the radiolabeled peptide) and, in the case of radioiodinated peptides, with potassium iodide (200 mg/d for 3 d), 4 patients with metastatic MTC were injected over a 10-min period with 370 MBq (10 mCi) ^{131}I-labeled gastrin-I (n = 1) or with 130–170 MBq (3.5–4.6 mCi) ^{111}In-DTPA-minigastrin (n = 3) (approximately 0.5 μg/kg body weight each). Whole-body scans and SPECT images of the thorax and abdomen were obtained over a 48-h period, using a

double-head gamma camera (Picker Prism 2000; Picker International) (11,12).

Statistical Analysis

Differences in the tissue uptake values and the biodistribution of the radioligands in various tissues were statistically analyzed with the Student t test for unpaired data. Pairwise comparisons were performed with the Wilcoxon rank-sum test. Differences in the therapeutic efficacy between the treatment modalities were analyzed by assuming an exponential tumor growth pattern; nonlinear regression analysis based on asymptotic approximation was used.

RESULTS

Stability and Affinity of the Various Peptides In Vitro

The peptides (Table 1) were radioiodinated by the Iodogen or Bolton-Hunter procedures as indicated, depending on the availability of a nonsubstituted tyrosyl moiety (Iodogen) or a free amino group (Bolton-Hunter). HPLC analysis of the radioiodinated peptides revealed a single peak ($\geq 95\%$ of the total activity) for Bolton-Hunter-labeled peptides in contrast to several (up to four) closely related peaks for their Iodogen-labeled analogs. Previous studies had shown that the methionine moieties of CCK or gastrin derivatives are readily susceptible to oxidation, even under rather mildly oxidizing conditions such as those occurring during Iodogen radioiodination. Accordingly, iodination of [Leu[15]]-gastrin-I, lacking any Met residues, led to a single ($\geq 95\%$ of the total activity) radioiodinated peptide.

To further study the role of methionine oxidation, redox experiments were undertaken by incubating the labeled peptides for 1 h at 37°C in 1-mol/L H_2O_2 or for 48 h in 1-mol/L dithiothreitol (21). HPLC analysis showed nearly complete interconversion of the various peptide peaks to a homogeneous product under each of these respective conditions. However, pilot receptor-binding studies failed to show any major influence of the methionine oxidation on the receptor-binding affinities (data not shown), which is in accordance with previous reports (25). Furthermore, pilot studies comparing the biodistribution of big-gastrin, minigastrin and nonsulfated CCK-8 labeled by the Iodogen (^{131}I) versus the Bolton-Hunter (^{125}I) procedure intraindividually did not show any significant difference between the biological behavior of both labels (data not shown). Therefore, the radiolabeled peptides were used for the subsequent studies without further consideration of partially oxidized Met residues.

Table 1 shows the IC_{50} values of the radioiodinated peptides obtained from cell-binding studies. Sulfated CCK and cionin analogs had the highest affinities ($\leq$nmol/L range), whereas desulfation or the complete removal of the N terminally located tyrosine-containing parts of the peptide (as is the case in des-BOC-pentagastrin or CCK-4) led to a loss of affinity by several orders of magnitude. Furthermore, the presence of an intact C-terminal Trp-Met-Asp-PheNH$_2$ sequence is crucial for receptor binding, whereas the methionine can be replaced by leucine or norleucine. Similarly high affinities as those seen for the sulfated CCK analogs were

observed for some nonsulfated members of the gastrin family.

Stability testing of the various peptides was performed in human serum. At 37°C, all peptides had in vitro serum half-lives of several hours, but those peptides bearing N-terminal pyroglutamic acid (pGlu) residues exhibited significantly longer half-lives ($\geq$24 h at 37°C) than those with a free N-terminal amino group (data not shown).

On HPLC analysis, a small fraction of the peptides ($\leq$10%) rapidly shifted to a higher molecular weight fraction on only a short serum incubation at 2°C, suggesting binding to serum proteins, whereas the majority of the peptides remained unbound. Incubation at 37°C led to small molecular weight metabolites, coeluting with di-, tri- or tetrapeptides or monoiodotyrosine (data not shown). A much more rapid metabolic breakdown of minigastrin was observed compared with the pGlu-protected gastrin-I. In addition, the replacement of the L-Leu^1-moiety in minigastrin by its D-isomer led to an improved serum stability ($t_{1/2}$ = 8 h versus 45 min at 37°C).

Biodistribution Studies in Human Medullary Thyroid Cancer Xenograft-Bearing Nude Mice

Biodistribution studies of the various peptides used were performed in TT xenograft-bearing nude mice. Figures 1 and 2 show the biodistribution patterns and the tissue uptake values, respectively, of those peptides essentially confined to the known receptor recognition region Trp-Met-Asp-PheNH$_2$ (e.g., CCK-4 and des-BOC-pentagastrin) and of the nonsulfated CCK analogs (nonsulfated CCK-8 and caerulein). Because similar biodistribution kinetics were observed for most members within each subfamily (e.g., nonsulfated versus sulfated CCK versus gastrin derivatives), Figures 1, 3 and 4 show the biodistribution of a typical member of the various families over a 24-h period (differentiating those tissues known or expected to express CCK-B receptors [top panels], organs involved in the excretion of the radiopeptide [middle panels] and pure "blood-pool" organs [bottom panels]), respectively. Furthermore, Figures 2, 5 and 6 quantitatively compare the tissue uptake of the most important tested peptides belonging to these families at 1-h postinjection. This time point was chosen because it was typically the time point with the highest target-specific uptake (Figs. 1, 3 and 4).

Accordingly, Figure 1 shows the biodistribution pattern of nonsulfated CCK derivatives. With nonsulfated CCK-8, over the first hour, increasing uptake was seen in the stomach (as the organ with the highest physiological CCK-B receptor density) (26) and the gallbladder as well as, in comparison with other tissues, some prolonged retention of activity in the tumor (Fig. 1, top panel). The major route of excretion was renal, with an initially intense uptake in the kidney (Fig. 1, middle panel). In addition to a potentially specific CCK receptor binding in the gallbladder, a biliary excretion pathway was suggested by an activity transfer into the bowel (Fig. 1, middle panel). All other organs studied, such as the lung, liver, spleen, muscle and bone, behaved as
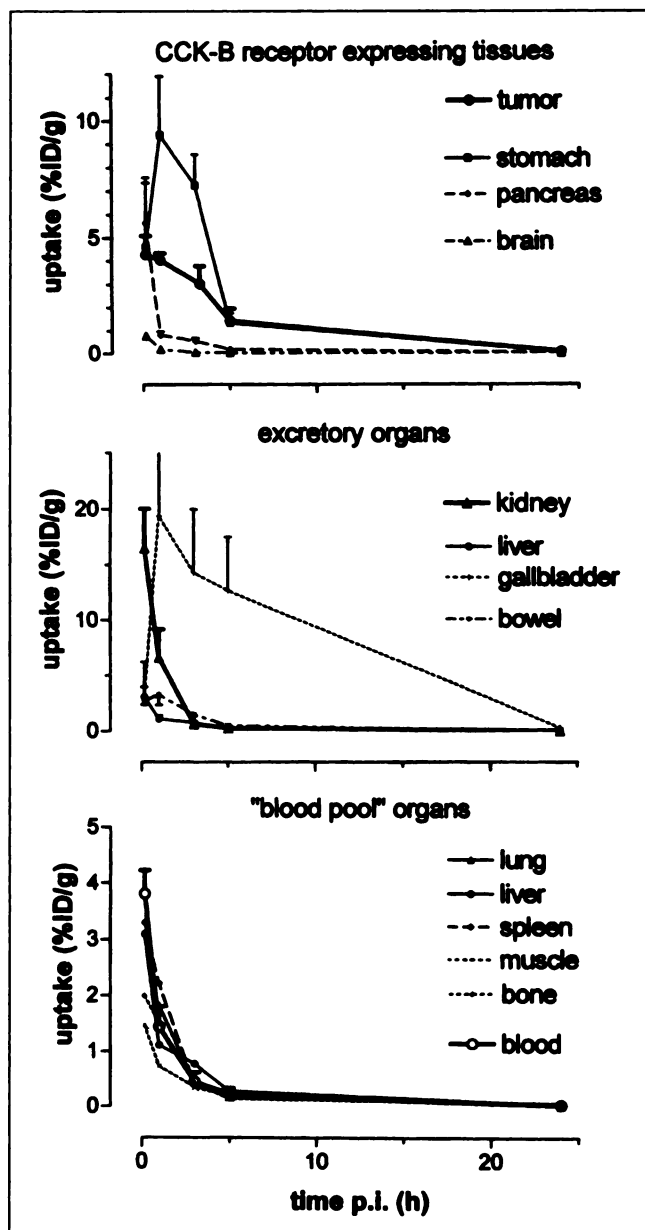

FIGURE 1. Biodistribution of nonsulfated CCK-8 in CCK-B receptor-expressing tissues (top), organs involved in its excretion (middle) and blood-pool organs (bottom) in time course.

typical blood-pool organs with a rapid, exponential clearance pattern that was parallel to the blood clearance (Fig. 1, bottom panel).

The comparison of the 1-h tissue uptake values of nonsulfated CCK-8 and nonsulfated caerulein with those of peptides essentially confined to the receptor-binding region, i.e., des-BOC-pentagastrin and CCK-4, shows hardly any stomach or tumor uptake with the latter, which is in contrast to the, although still rather low, significantly (P < 0.05) higher uptake of nonsulfated CCK-8 and caerulein in these tissues. This is in accordance with the external scintigraphy (Fig. 7, first scan), which shows hardly any tumor and only rather weak stomach uptake for nonsulfated CCK-8 as the organs with the highest CCK receptor expression (mainly
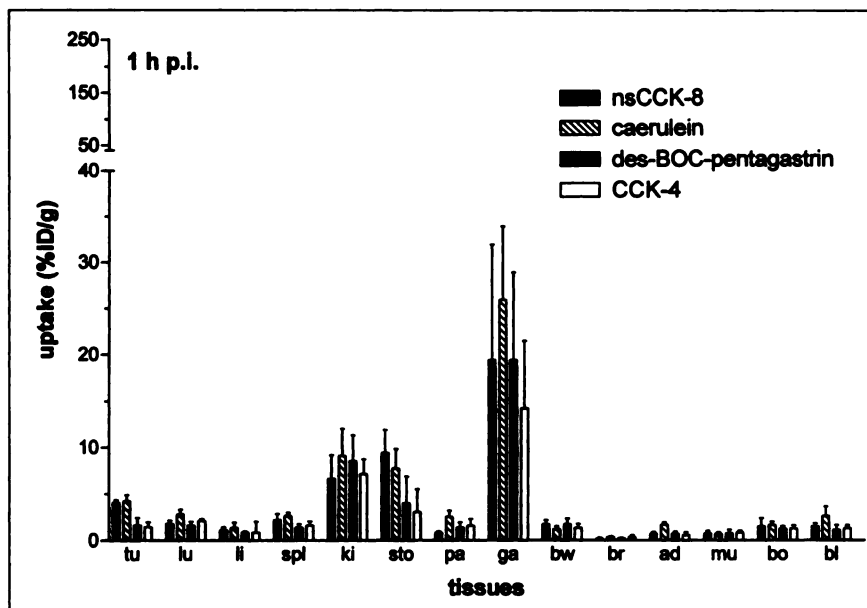
FIGURE 2. Comparison of 1 h postinjection tissue uptake values of radioiodinated nonsulfated CCK-8 (nsCCK-8), caerulein, des-BOC-pentagastrin and CCK-4. tu = tumor; lu = lung; li = liver; spl = spleen; ki = kidney; sto = stomach; pa = pancreas; ga = gallbladder; bw = bowel; br = brain; ad = adrenal gland; mu = muscle; bo = bone; bl = blood.

visualization of the kidneys and gallbladder as excretory organs).

Figure 3 shows the biodistribution pattern of typical sulfated members of the CCK family and of bisulfated cionin as a peptide with characteristics common to both the CCK and gastrin families. As an example, Figures 3 and 7 (second scan) depict the biodistribution of sulfated CCK-8 in TT-bearing nude mice. Significantly higher uptake and longer retention times than with their nonsulfated analogs were observed in the tumor, stomach, gallbladder and pancreas ($P \leq 0.03$; Figs. 1 and 3), which is reflected by a better external scintigraphic visualization of these tissues (Fig. 7). However, uptake also occurred in the liver and bowel, whereas the renal accretion of sulfated compounds was significantly lower than that with their nonsulfated analogs. Figure 5 shows that all three sulfated compounds that conserve the Trp-Met-Asp-PheNH$_2$ sequence or its Nle analog (i.e., sulfated CCK-8, [Thr^{28},Nle^{31}]-sCCK-25–33 and cionin) had very similar biodistribution patterns, whereas the uptake values of [Tyr(SO$_3$H)^{27}]-CCK-26–29, lacking the receptor-binding tetrapeptide, were significantly lower in the CCK-B receptor-expressing tissues (e.g., tumor, stomach and pancreas; $P \leq 0.02$), as well as in the gallbladder and bowel.

Figure 4 shows the biodistribution of radiolabeled members of the gastrin family, and Figure 7 (third scan) depicts the biodistribution of gastrin-I as a typical representative. Similar to the sulfated CCK derivatives, over the first hour, increasing uptake was seen in the tumor and stomach (Fig. 4, upper panel). In contrast to the sulfated CCK analogs, the liver uptake was significantly lower ($P < 0.02$), whereas the renal accretion and retention were considerably higher (Figs. 3 and 4). No significant differences were observed in the biodistribution patterns of gastrin-I, its [Leu^{15}]-analog and minigastrin, with the exception of the kidney, in which the retention of the latter was significantly lower than that

observed with gastrin-I or its [Leu^{15}]-analog (Fig. 6). In contrast, big-gastrin showed a significantly lower uptake in the tumor, stomach and other potentially CCK-B receptor-expressing tissues, whereas its blood clearance was slower, and its kidney uptake was approximately four times higher than that observed with any other gastrin analog (Fig. 6).

Because high affinity to the CCK-B receptor and good target organ (i.e., stomach and tumor) uptake were observed with both the sulfated CCK and the anionic pentaglutamate sequence containing gastrin analogs, we hypothesized that these negative charges might be involved in receptor binding and affinity. Therefore, we examined the biodistribution of polar but neutral gastrin analogs, [Gln$_5$$^{6-10}$]-gastrin-I and [Gln$_5$$^{2-6}$]-minigastrin. Indeed, the tumor and stomach uptakes were significantly ($P < 0.03$) lower than those with gastrin-I or minigastrin, as was also the case for the renal accretion (Figs. 6 and 7, fourth scan). Again, no significant difference was observed between the biodistributions of both Gln$_5$-peptides (biodistribution data for [Gln$_5$$^{6-10}$]-gastrin-I not shown). Whereas with members of the gastrin family, excellent visualization of the tumor and normal CCK-B receptor-expressing tissues was seen (Fig. 7, third scan), the replacement of the pentaglutamate sequence, as in [Gln$_5$$^{6-10}$]-gastrin-I, led to a significantly decreased CCK-B receptor-mediated tumor and stomach uptake (Figs. 6 and 7, fourth scan). The best stomach-to-normal-organ ratios were obtained with sulfated CCK or cionin derivatives (Table 2). However, because of their lower accretion in CCK-A-expressing abdominal organs, the best tumor-to-nontumor ratios were obtained with members of the gastrin family, especially gastrin-I, its [Leu^{15}] analog or minigastrin (Table 2).

The specificity of receptor-targeted uptake in various tissues was assessed by comparing the biodistribution of 1 µg radioiodinated gastrin-I with the 1000-fold higher peptide amount by coinjecting 1 mg unlabeled gastrin-I (Figs. 8

and 9). The uptake in the tumor, stomach and pancreas was significantly lower at the 1-mg saturation dose. Interestingly, despite receptor blocking, the gallbladder uptake was still quite substantial, indicating that this uptake may be due to nonspecific biliary excretion. Surprisingly, the renal accretion was lowered under receptor saturation conditions as well ($P < 0.05$), whereas the blood clearance seemed to be slightly slower under high-dose peptide challenge conditions. No significant differences were found in lung, liver, spleen, bowel, brain, adrenal, muscle or bone uptakes. In addition, the biodistribution of fragment 1–14, lacking an intact C-terminal receptor-binding tetrapeptide, was studied
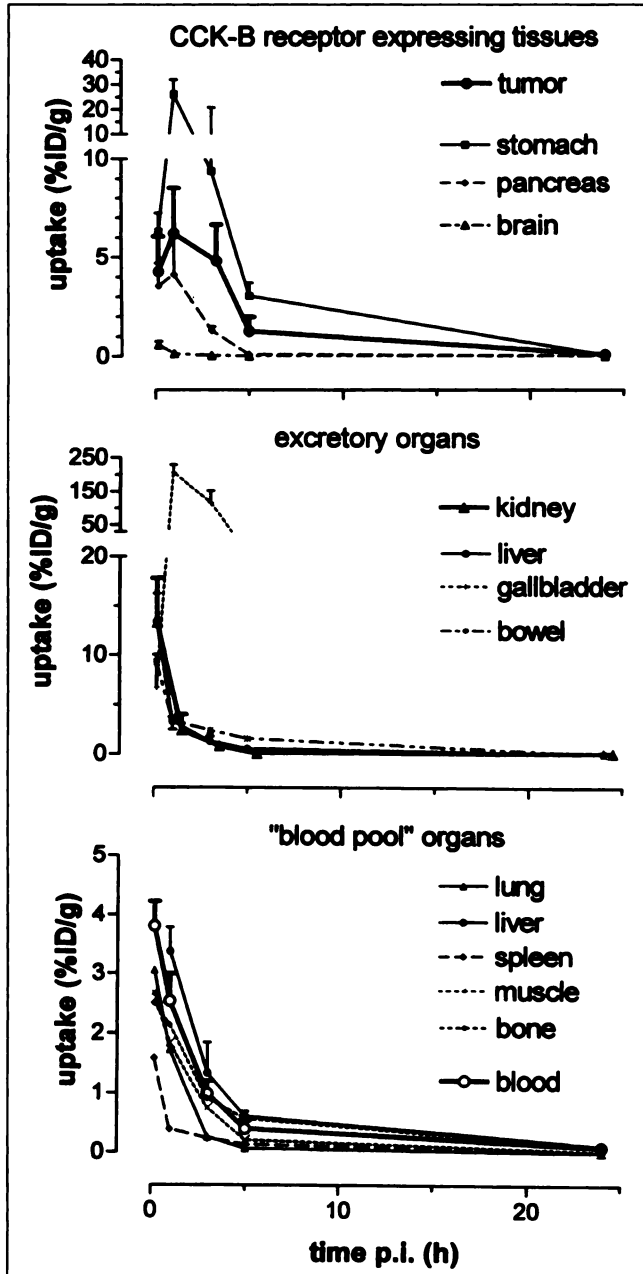
FIGURE 3. Biodistribution of sulfated CCK-8 in CCK-B receptor-expressing tissues (top), organs involved in its excretion (middle) and blood-pool organs (bottom) in time course.
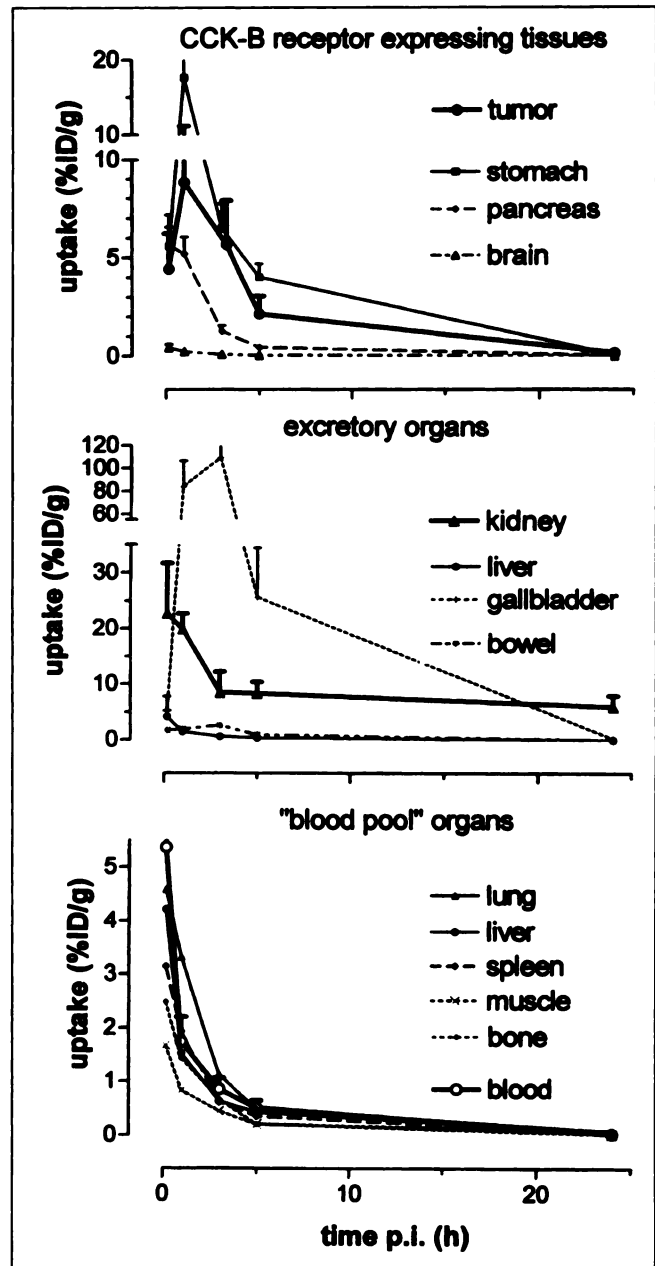

FIGURE 4. Biodistribution of gastrin-I in CCK-B receptor-expressing tissues (top), organs involved in its excretion (middle) and blood-pool organs (bottom) in time course.

(Fig. 8). Again, significantly lower uptake of this peptide occurred in the tumor, stomach and pancreas ($P < 0.01$), whereas there was no difference in the renal accretion of gastrin-I.

Observations on the Influence of Molecular Characteristics on Renal Accretion

Figure 10 shows the kidney accretion dynamics for nonsulfated (top panel) and sulfated (middle panel) CCK analogs and members of the gastrin family (bottom panel). Whereas the initial renal uptake and retention of the sulfated, thus highly anionic, CCK analogs (middle panel) were very low, the initial uptake of their nonsulfated analogs was

FIGURE 5. Comparison of 1 h postinjection tissue uptake values of radioiodinated sulfated CCK-8 (sCCK-8), [Thr^{28},Nle^{31}]-sCCK-25–33, cionin and [Tyr(SO$_3$H)^{27}]-CCK-26–29. tu = tumor; lu = lung; li = liver; spl = spleen; ki = kidney; sto = stomach; pa = pancreas; ga = gallbladder; bw = bowel; br = brain; ad = adrenal gland; mu = muscle; bo = bone; bl = blood.
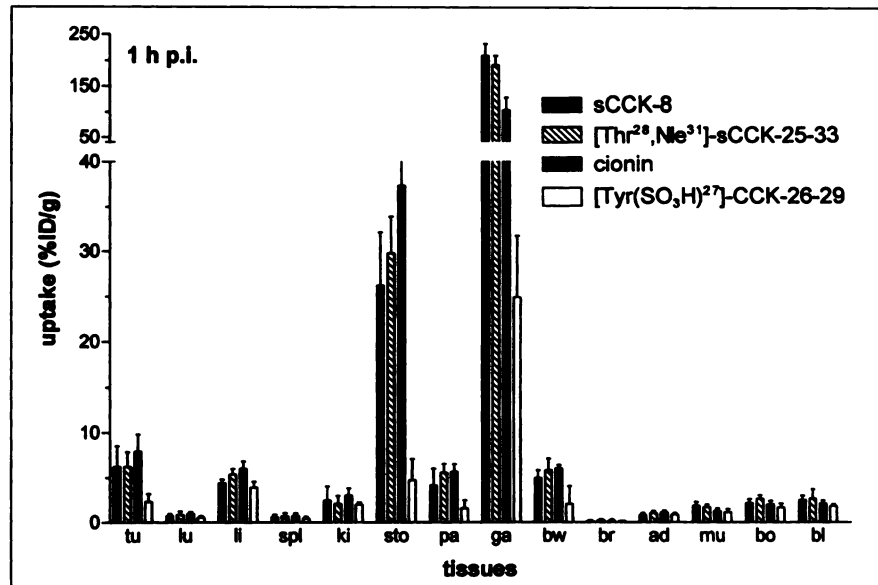
approximately twofold higher (top and middle panels), which held true for members of the gastrin family (bottom panel) as well. The retention of peptides bearing an N-terminal pGlu moiety was significantly longer (dashed lines in Fig. 10) than with "open-ended" peptides (various dotted lines in Fig. 10). Finally, big-gastrin, which is the only peptide with two positively charged lysine groups and an N-terminal pGlu moiety, had the highest renal uptake and longest retention of all peptides studied.

Initial Therapeutic Experiments with ^{131}I-Labeled Gastrin Analogs

Because of the encouraging "diagnostic" results of CCK-B receptor targeting, we undertook initial experiments to assess whether radiolabeled gastrin may be therapeutically useful. To determine the maximum tolerated dose and dose-limiting organs, varying amounts of gastrin-I or its

fragment 1–14 were injected into groups of 10 animals each, starting at 74 MBq (2 mCi) and increasing in 10%–20% steps. Myelotoxicity was found to be dose-limiting (blood count nadirs at 1- to 2-wk postinjection, complete recovery within 2–3 wk) with both ^{131}I-labeled peptides, and the maximum tolerated activity was reached at 170 MBq (4.5 mCi), corresponding to a blood dose of approximately 3.5 Gy (12). No sign of second-organ toxicity was observed; values for blood urea nitrogen, creatinine and the liver enzymes remained within normal limits. This is in contrast to big-gastrin, in which we observed signs of radiation nephrotoxicity (rising blood urea nitrogen and creatinine levels; data not shown), which is in accordance with its higher renal accretion and retention. The tumor growth was significantly retarded with ^{131}I-gastrin-I ($P = 0.03$) compared with untreated controls, with animals given the same

FIGURE 6. Comparison of 1 h postinjection tissue uptake values of radioiodinated big-gastrin, gastrin-I, [Leu^{15}]-gastrin-I, minigastrin and [Gln$_5^{2-6}$]-minigastrin. tu = tumor; lu = lung; li = liver; spl = spleen; ki = kidney; sto = stomach; pa = pancreas; ga = gallbladder; bw = bowel; br = brain; ad = adrenal gland; mu = muscle; bo = bone; bl = blood.
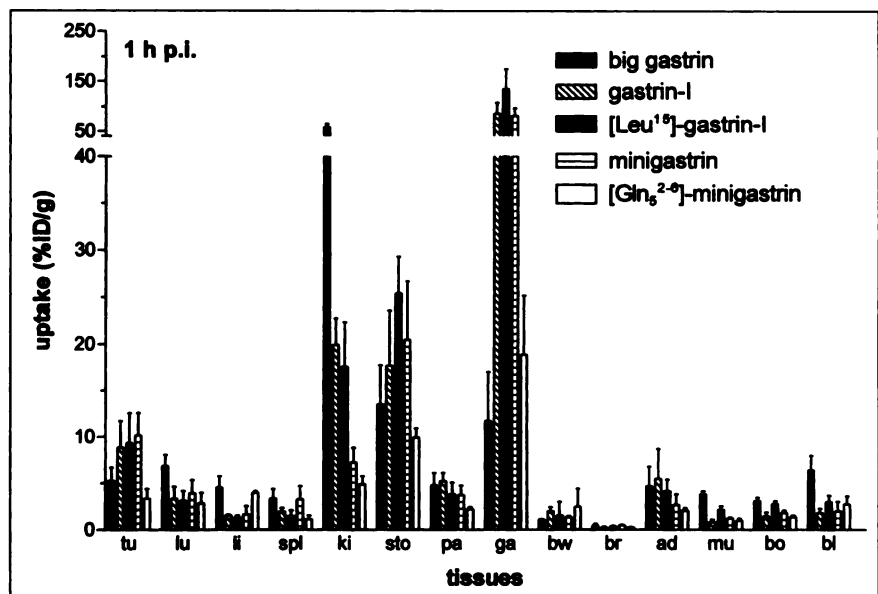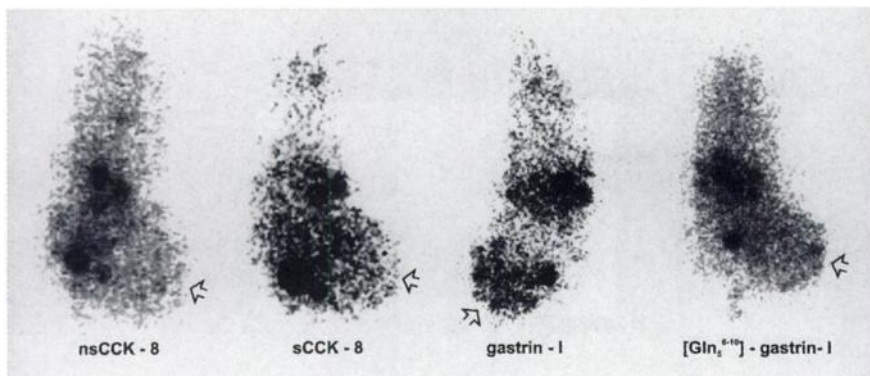
FIGURE 7. Scintigrams of subcutaneously TT-xenografted nude mice at 1 h postinjection (Picker Prism 2000 gamma camera equipped with high-energy, parallel-hole collimators; 100 kcts each): nonsulfated (ns) versus sulfated (s) CCK-8, gastrin-I versus [Gln_5^{6-10}]-gastrin-I. Arrows designate tumor in each animal (ventral views each).

amount of unlabeled peptide or with animals given ^{131}I-labeled fragment 1–14 as irrelevant peptide (Fig. 11).

Development of an ^{111}In-Labeled Cholecystokinin-B Receptor-Binding Peptide

On the basis of the results presented thus far, gastrin analogs containing the highly anionic Glu_5 sequence, together with the receptor-binding C-terminal tetrapeptide Trp-Met-Asp-PheNH$_2$, seem to combine high affinity and selectivity for the CCK-B receptor with a relatively low renal accretion. Therefore, minigastrin and its [D-Leu^1] analog were chosen as the basis for developing an ^{111}In-labeled CCK-B receptor-imaging agent for potential clinical purposes. As described in more detail in the Materials and Methods section, a DTPA derivative was synthesized. HPLC

analysis demonstrated a single peptide that could be labeled with ^{111}In at a specific activity of ≥18.5 MBq/µg (0.5 mCi/µg) with >98% radiochemical purity without requiring additional postlabeling purification. The biodistribution of ^{111}In-DTPA-minigastrin in TT-bearing nude mice is shown in Figures 12 and 13. The peptide showed a maximum tumor uptake of 5.0 ± 1.2 %ID/g and a stomach uptake of 9.4 ± 2.7 %ID/g at 1 h postinjection. It had a rapid clearance from the blood and blood-pool organs (lungs, liver, spleen, muscle and bone), with mainly renal (maximum kidney uptake of approximately 45 %ID/g) and some biliary excretion (transient gallbladder uptake with activity transfer into the bowel). In contrast to radioiodinated minigastrin, a prolonged retention in the adrenals was observed with its

TABLE 2
Mean Target-to-Background Ratios at 1 hour Postinjection for Most Important Cholecystokinin (CCK)-B Receptor-Expressing Tissues for Various Radioiodinated Peptides

Peptide (family)	Tumor							Stomach						
	Blood	Lung	Liver	Pancr.	Gallbl.	Bowel	Kidney	Blood	Lung	Liver	Pancr.	Gallbl.	Bowel	Kidney
Gastrin derivatives														
Big-gastrin	1.2	1.4	1.2	1.1	0.4	4.7	0.1	2.1	2.0	3.0	2.8	1.2	12.2	0.2
Gastrin-I	4.9	2.8	5.8	1.7	0.1	4.4	0.4	9.8	5.3	11.5	3.4	0.2	8.9	0.9
[Leu^{15}]-gastrin-I	3.7	3.0	7.0	2.5	0.1	4.4	0.4	8.5	8.1	22.0	6.7	0.2	16.9	1.5
[Gln_5^{6-10}]-gastrin-I	1.1	1.2	0.7	1.3	0.2	1.3	0.7	6.5	3.4	1.9	4.0	0.5	2.9	2.3
Minigastrin	5.1	2.6	6.2	2.7	0.1	7.5	1.4	10.4	5.2	6.1	5.5	0.3	15.1	2.8
[Gln_5^{2-6}]-minigastrin	1.2	1.2	0.8	1.5	0.2	1.4	0.7	6.9	3.5	2.5	4.5	0.5	4.0	2.0
Gastrin-I fragment 11–17	2.0	2.3	3.8	4.9	0.2	2.4	0.6	3.1	4.3	6.4	8.3	0.4	4.4	1.2
Gastrin-I fragment 1–14	1.1	1.0	1.9	0.8	0.1	2.1	0.2	2.9	2.8	5.2	2.2	0.1	5.9	0.5
CCK derivatives														
Caerulein	1.6	1.5	3.1	1.7	0.2	3.5	0.5	2.9	2.7	5.7	3.0	0.3	6.4	0.9
[Thr^{28},Nle^{31}]-sCCK-25-33	2.4	7.2	1.2	1.1	<0.1	1.1	3.0	11.3	34.2	5.5	5.3	0.2	5.1	14.2
sCCK-8	2.7	8.5	1.4	1.5	<0.1	1.2	2.5	10.5	35.9	6.0	6.3	0.1	5.3	10.5
nsCCK-8	2.5	2.1	3.6	5.0	0.2	2.3	0.6	6.3	5.1	8.4	11.6	0.5	5.4	1.4
[Tyr(SO$_3$H)^{27}] CCK 26–29	1.3	4.3	0.6	1.5	0.1	1.2	1.2	2.6	8.7	1.2	2.9	0.2	2.3	2.4
Peptides with common features of both gastrin and CCK														
Cionin	3.6	8.3	1.3	1.4	0.1	1.3	2.6	17.8	28.0	6.2	4.6	0.4	6.2	12.4
des-BOC-pentagastrin	1.5	1.0	1.9	1.2	0.1	0.9	0.9	3.6	2.5	4.8	2.9	0.2	2.3	0.5
CCK fragment 30–33 (CCK-4)	1.1	0.7	1.7	0.9	0.1	1.1	0.2	2.4	1.5	3.6	2.0	0.2	2.3	0.4

Pancr. = pancreas; Gallbl. = gallbladder.

FIGURE 8. Specificity of CCK-B receptor binding. Comparison of biodistribution of 1 µg ^{131}I-labeled gastrin-I versus 1 µg radiolabeled gastrin, supplemented with 1 mg unlabeled peptide or 1 µg fragment (fragm.) 1–14 (lacking receptor-binding tetrapeptide sequence). *P < 0.05; **P < 0.01; tu = tumor; lu = lung; li = liver; spl = spleen; ki = kidney; sto = stomach; pa = pancreas; ga = gallbladder; bw = bowel; br = brain; ad = adrenal gland; mu = muscle; bo = bone; bl = blood.
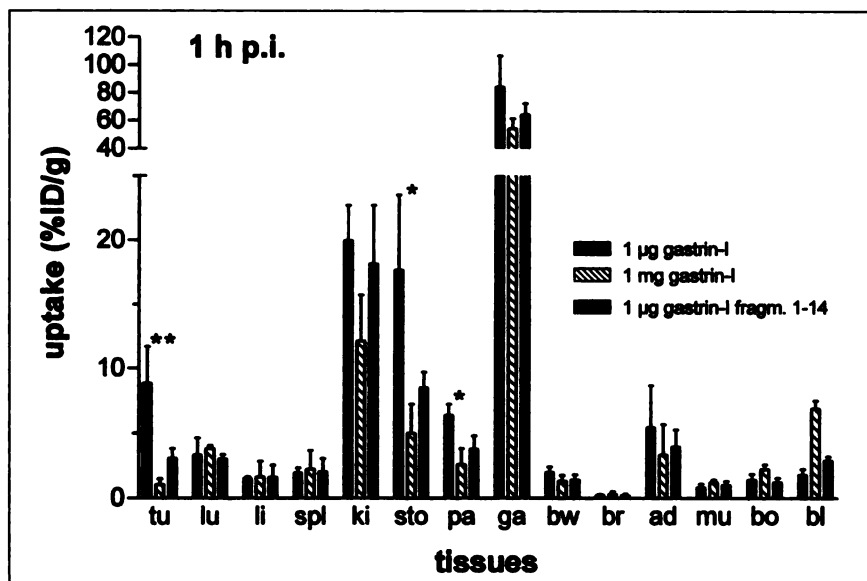
^{111}In-labeled derivative. No significant difference was observed between ^{111}In-DTPA-minigastrin and its [D-Leu^1] analog (data not shown).

Pilot Clinical Evaluation of ^{131}I-Labeled Gastrin-I and ^{111}In-DTPA-Minigastrin

Four patients with known or occult metastatic MTC were investigated with either ^{131}I-labeled gastrin-I (one patient) or ^{111}In-DTPA-minigastrin (three patients) (Table 3). Three patients had known lesions, and one patient had occult

FIGURE 9. External scintigram comparing 1 µg ^{131}I-labeled gastrin-I (left) with 1 mg blocking dose (right).

metastatic MTC, as indicated by pathologically elevated carcinoembryonic antigen (CEA) and calcitonin levels without radiological evidence of disease. All patients had undergone somatostatin receptor and anti-CEA immunoscintigraphy within 3 mo. A peptide dose of 0.5 µg/kg body weight was slowly injected intravenously, which was tolerated by two patients without any side effects, whereas the other two patients had a short episode of pentagastrin stimulation-test-like symptoms (nausea, "strange feeling" in the abdomen), lasting for only a few minutes and resolving spontaneously. In accordance with the preclinical studies, receptor targeting was seen in all four patients in physiologically CCK-B receptor-expressing tissues (mainly in the stomach), as well as in all known metastatic lesions (Table 3 and Figs. 14 and 15). In the second patient with occult metastatic MTC (without evidence of disease on somatostatin or anti-CEA scintigraphy), ^{111}In-DTPA-minigastrin detected a previously occult liver lesion that was confirmed by CT 4 wk later, whereas splenic involvement that was suspected by ^{111}In-DTPA-minigastrin scanning remained unconfirmed positive.
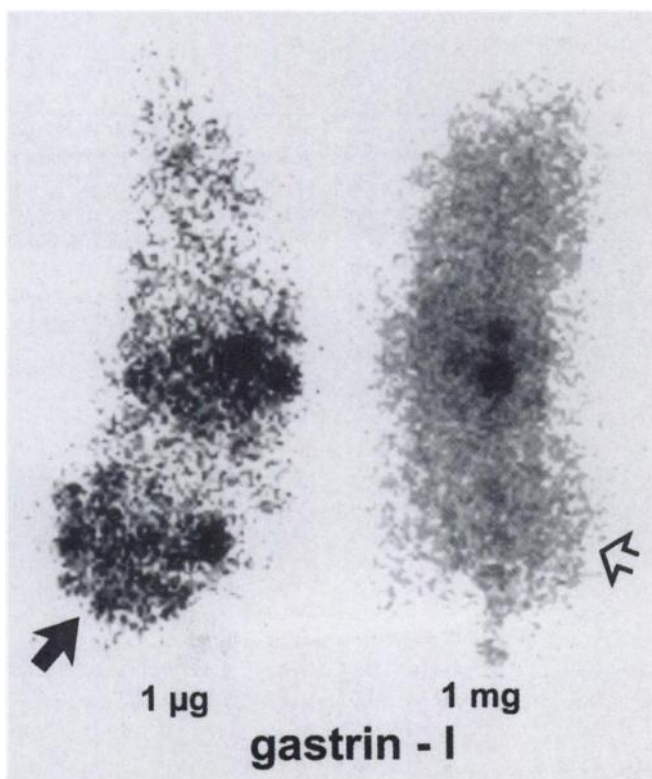
DISCUSSION

The outstanding sensitivity of pentagastrin in detecting the presence of malignant C cells suggests the expression of a corresponding receptor type in human MTC (27). Indeed, receptor autoradiographic studies by Reubi and Waser (13) and Reubi et al. (14) have demonstrated the presence of CCK-B/gastrin in more than 90% of MTCs and in a high percentage of other important tumor types, such as small cell lung cancer, stromal ovarian cancers and astrocytomas. Even though the expression of relevant amounts of CCK-B receptors in typical adenocarcinomas is a matter of debate, some investigators were able to demonstrate and characterize this receptor type in colon, gastric and pancreatic cancers
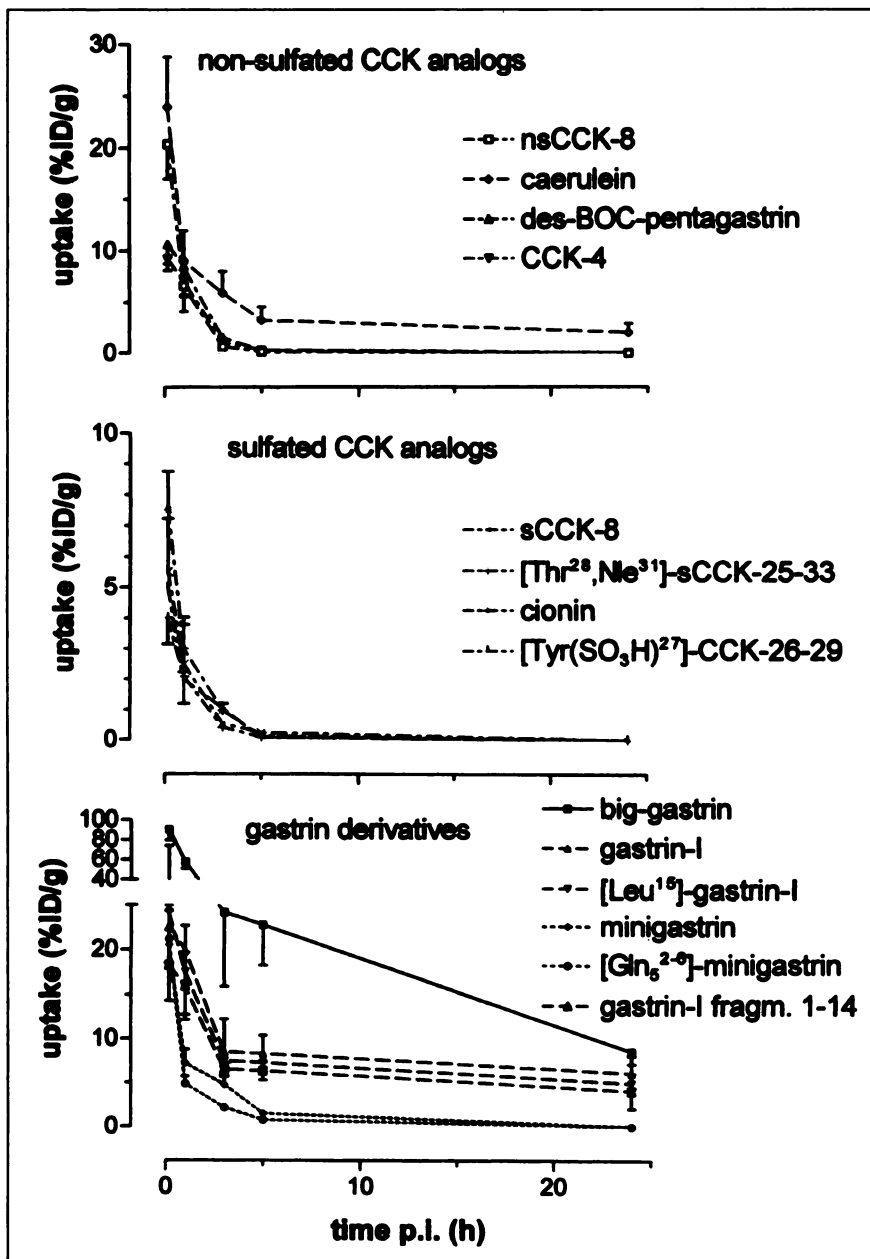
FIGURE 10. Comparison of biokinetics of various peptides in kidneys for nonsulfated (top) and sulfated (middle) CCK analogs and members of gastrin family (bottom). Solid lines represent peptides containing cationic amino acids (lysine), dashed lines represent peptides with N-terminal pGlu moiety and various dotted lines represent peptides lacking both of these characteristics.

as well (15). Thus, there are ample reasons to regard CCK-B receptors as an attractive target for radiolabeled peptides for diagnostic and therapeutic purposes.

Although we were previously able to demonstrate the feasibility of radiolabeled gastrin-I to target CCK-B receptor-expressing tissues in animals and patients (12), a variety of problems remained unsolved to identify an optimum candidate for in vivo targeting of CCK-B receptor-expressing tumors in larger clinical studies. The aim of this study, therefore, was to develop and optimize suitable radioligands for targeting CCK receptors in vivo.

Previous studies had provided evidence for an unusual susceptibility of the methionine moieties of CCK and gastrin derivatives toward oxidation, e.g., during radioiodination. Our data seem to confirm this sensitivity, but, in accordance

with previous results (25), they also seem to confirm that (at least partial) oxidation of the Met residues (e.g., to methionine sulfoxide) does not affect the receptor-binding capabilities of these radioiodinated peptides. Accordingly, no significant differences in biodistribution were noticed, whether using peptides labeled according to the Bolton-Hunter or the Iodogen procedure.

Because standard methods for determining the binding affinity of peptides use either quantitative receptor autoradiography in frozen tissue sections or cortex membrane preparations, our data obtained by a different methodology were intended to provide only rough estimates. That is why only the approximate orders of magnitude are given in Table 1. Nevertheless, the values obtained are in accordance with published values (28,29). Our affinity/IC_{50} results show that
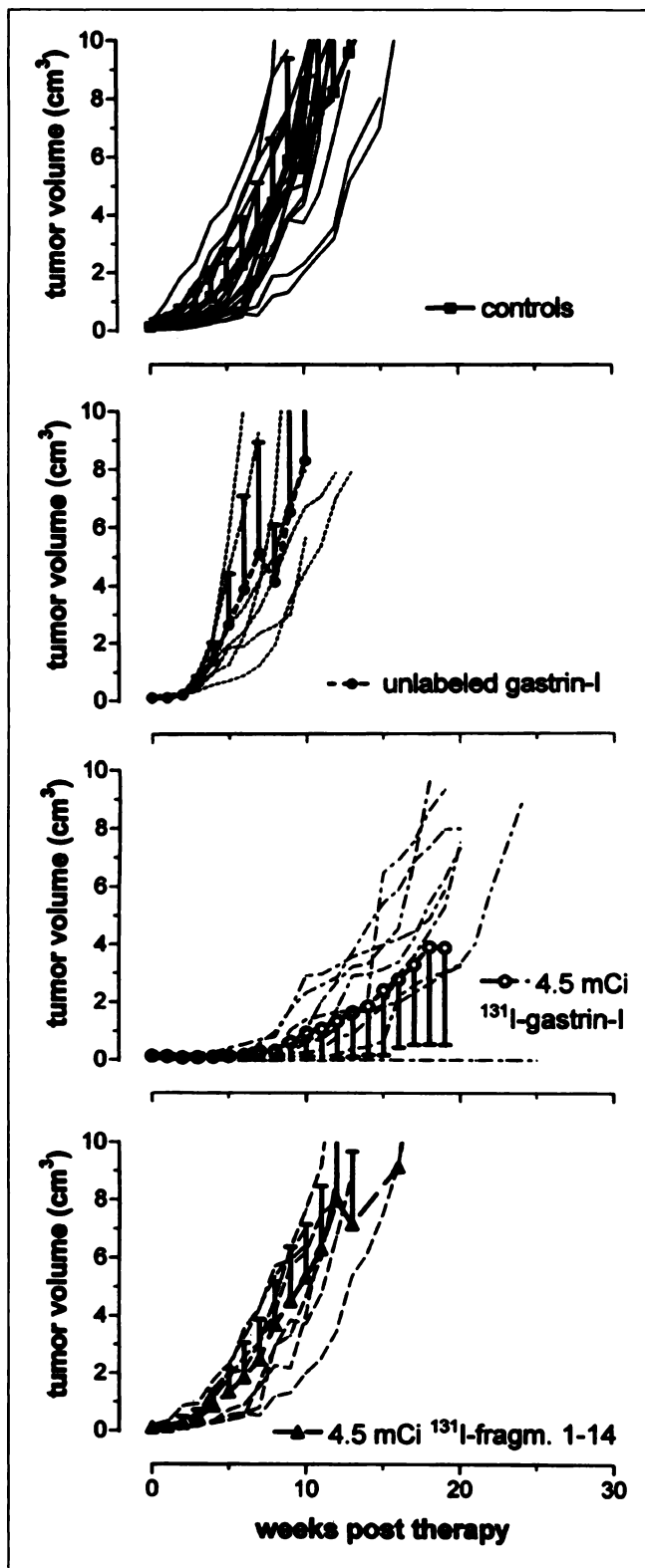
FIGURE 11. Therapeutic efficacy of ^{131}I-labeled gastrin-I at its maximum tolerated dose of 167 MBq (4.5 mCi) compared with untreated controls, animals given same amount of unlabeled gastrin-I and 167 MBq fragment (fragm.) 1–14 (difference between ^{131}I-gastrin-I and other groups statistically significant at $P = 0.03$).

important requirements for a high affinity to the CCK-B receptor are the presence of the C-terminal tetrapeptide sequence Trp-Met-Asp-PheNH$_2$ (in which Met can be replaced by Nle or Leu) and either a sulfated tyrosine moiety (as is the case in sulfated CCK derivatives) or the presence of a Glu$_5$ sequence adjacent to a nonsulfated Tyr residue (as is the case in the gastrin family). In contrast, nonsulfated CCK analogs showed a considerably decreased affinity.

In contrast to most of regulatory peptides, CCK or gastrin derivatives seem to be fairly stable in serum. The major biological inactivation pathway is known to be renal filtration and enzymatic degradation (*30*). With half-lives of several hours, it did not seem necessary to introduce special stabilizing functional groups or molecular modifications, as had been the case in the development of somatostatin analogs (*31*). The protective effect of N-terminal pGlu residues against serum peptidase action is a well-known phenomenon (*31*) and could be demonstrated in this study as well. Although there are known "gastrin-binding" proteins in the serum (*32*), our data clearly suggest that the vast majority of CCK or gastrin analogs circulate as free peptides, which seems to be an important prerequisite for rapid receptor targeting and background clearance.

As has been expected from the interspecies similarity of peptides of the CCK/gastrin families and their receptors (*28,29*), the biodistribution studies of human gastrin in nude mice showed specific binding to the tumor and most organs known to express CCK-B receptors. The lack of uptake in the brain (despite the known presence of CCK-B receptors) (*28*) is easily explained by the inability of the hydrophilic peptide to cross the blood-brain barrier. Furthermore, the biodistribution studies in MTC-xenografted nude mice clearly demonstrate that the requirements of a peptide to yield reasonably good uptake in CCK-B receptor-expressing tissues and, in addition, to yield sufficiently high target-to-background ratios are to bear the C-terminal tetrapeptide sequence Trp-Met-Asp-PheNH$_2$ (in which Met may be substituted by Leu or Nle) and to contain either a sulfated tyrosyl moiety or a highly anionic oligo-(penta?)-glutamate sequence in its N-terminal neighborhood. It is a well-established phenomenon that a sulfated tyrosyl moiety is a crucial requirement for the affinity of a peptide to the CCK-A receptor, whereas in the case of CCK-B receptors, both sulfated CCK and (nonsulfated) gastrin derivatives have shown similar affinities (*28,29*). Our hypothesis regarding the importance of the pentaglutamate sequence in the gastrin-related peptides for its receptor-binding properties was supported by the comparably low affinity and poor receptor-targeting properties of the two synthetic peptides, in which the anionic Glu residues have been replaced by similarly polar but uncharged Gln moieties ([Gln$_5$$^{6-10}$]-gastrin-I and [Gln$_5$$^{2-6}$]-minigastrin; Figs. 4, 6 and 7). The comparably weak performance of big-gastrin may be due to the presence of two lysine moieties, which, on the one hand, may partially neutralize negative charges of the pentaglutamate sequence involved in receptor binding and, on the other
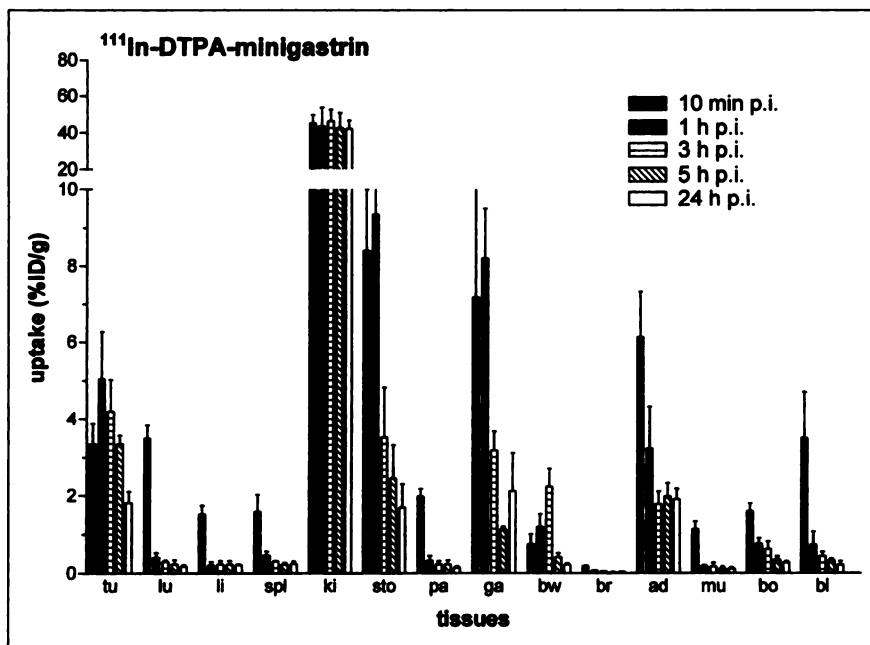
FIGURE 12. Quantitative biodistribution of ^{111}In-DTPA-minigastrin. tu = tumor; lu = lung; li = liver; spl = spleen; ki = kidney; sto = stomach; pa = pancreas; ga = gallbladder; bw = bowel; br = brain; ad = adrenal gland; mu = muscle; bo = bone; bl = blood.

hand, are known to contribute to the renal tubular reabsorption of peptides and low-molecular-weight proteins (*33,34*).

In accordance with their high affinity to the CCK-A receptor, which is almost ubiquitously present throughout the gastrointestinal tract (especially in the pancreatic acini and islets, the gallbladder, neurons and smooth muscle cells throughout the bowel, as well as gastric mucosal cells) (*35*), sulfated CCK analogs showed high uptake not only in the stomach but also in the bowel, pancreas, liver and gallbladder. Therefore, we postulate that for high affinity to and selectivity for the CCK-B receptor, nonsulfated gastrin derivatives may be superior to CCK analogs, the latter

FIGURE 13. External scintigram of subcutaneously TT-xenografted nude mouse at 1 h postinjection of ^{111}In-DTPA-minigastrin (Picker Prism 2000 gamma camera, medium-energy, parallel-hole collimators; 100 kcts). Arrow designates tumor (ventral view).

having been proposed for CCK-B receptor visualization in vivo by Reubi et al. (*36*).

The main excretion pathways of gastrin and CCK-related peptides seem to be renal filtration and, to a lesser extent, biliary excretion. Interestingly, the molecular structure of the various peptides was also reflected by their renal handling. The highest renal accretion occurred with big-gastrin, which is the only peptide studied that bears positively charged lysine residues. The latter are known to be involved in renal tubular reabsorption (*33,34*). In contrast, the sulfated, thus strongly anionic, CCK derivatives showed the lowest renal uptake and retention of all peptides studied. In contrast, N-terminal pGlu moieties seem to protect not only from serum peptidase digestion but also from lysosomal degradation in the renal tubuli, because peptides bearing such N-terminal pGlu moieties had longer activity retention in the kidneys than their "open-chained" counterparts (Fig. 10).

Because these data identify the amino acid sequence ... -(Glu)$_n$-X-Tyr-(Y)$_{1-2}$-Trp-Met-Asp-PheNH$_2$ (where X and Y may be any neutral amino acid, such as Ala, Gly or Thr; Met may be replaced by Leu or Nle; and n = 5, but other chain lengths remain to be tested) as the basic structure combining selectivity for and high affinity to the CCK-B receptor, we embarked on developing CCK-B receptor-targeting peptides, which are suitable for labeling with radiometals, such as ^{111}In. Such a peptide appears to be much more convenient for clinical purposes because of the more favorable physical imaging characteristics of indium compared with iodine and because of an anticipated easier labeling formulation. In addition, because indication for an internalization of CCK-B receptor ligands exists (*37*), residualizing radiolabels, such as radiometals, may be expected to improve tumor-to-nontumor ratios over rapidly

| Patient	History	Known lesions at time of presentation	Tumor marker levels		Scintigraphic diagnosis with gastrin analogs
71-y-old man	Spontaneous MTC (pT4 pN1 M1) 3 mo earlier	Bilateral hilar lymph node and lung metastases	CEA Calcitonin	95.9 ng/mL 4,417 ng/L	370 MBq (10 mCi) ^{131}I-gastrin-I: bilateral hilar lymph node and lung metastases
50-y-old man	Spontaneous MTC (pT3 pN1 M0) 7 y earlier	None (occult metastatic MTC)	CEA Calcitonin	18.3 ng/mL 6,582 ng/L	130 MBq (3.5 mCi) ^{111}In-DTPA-minigastrin: liver metastasis, questionable splenic involvement
43-y-old man	MEN 2A syndrome MTC (TNM?) 14 y earlier	Left hilar lymph node involvement	CEA Calcitonin	65.6 ng/mL 11,502 ng/L	133 MBq (3.6 mCi) ^{111}In-DTPA-minigastrin: left hilar lymph node metastasis
33-y-old man	MEN 2B syndrome MTC (TNM?) 7 y earlier	Cervical lymph node, lung metastases	CEA Calcitonin	296.8 ng/mL 34,508 ng/L	170 MBq (4.6 mCi) ^{111}In-DTPA-minigastrin: cervical and mediastinal lymph node, lung, liver and bone metastases

MTC = medullary thyroid cancer; CEA = carcinoembryonic antigen; MEN = multiple endocrine neoplasia.

released labels, such as conventional iodination (*38*). The DTPA derivative of minigastrin tested in this study seems to fulfill all these requirements. The animal biodistribution data show good targeting of CCK-B receptor-expressing tissues (mainly tumor and stomach) and more prolonged retention of the activity in these tissues (Figs. 4 and 12) than with iodine. Interestingly, in contrast to our observations with radioiodinated gastrin analogs, ^{111}In-DTPA-minigastrin seems to exhibit some increased adrenal uptake. Future studies will have to address whether this is due to receptor-specific binding (as is the case for somatostatin analogs in rodent adrenals) or merely to nonspecific processes.

In accordance with these preclinical data on the favorable targeting properties of ^{111}In-DTPA-minigastrin, our pilot clinical data confirm that this peptide is capable of targeting physiological (e.g., in the stomach) and pathological CCK-B receptor expressing tissues (e.g., in tumors). This is in accordance with previous data showing that phylogenetic differences concerning the receptor affinity toward human gastrin-I, at least between mammalian species, are minimal (*28,29*). Interestingly, the liver uptake of ^{111}In-DTPA-minigastrin seems to be considerably lower than that observed with ^{111}In-DTPA-pentetreotide (Figs. 14 and 15), which may favor the detection of liver metastases. Accordingly, in one patient with occult metastatic disease, ^{111}In-DTPA-minigastrin was able to demonstrate a liver metastasis that only became detectable by CT 1 mo later. Further clinical studies are warranted to show whether radiolabeled

FIGURE 14. Targeting of CCK-B compared with somatostatin receptors in 43-y-old man with MTC in connection with multiple endocrine neoplasia type 2A (patient 3, Table 3). ^{111}In-DTPA-minigastrin whole-body scan (left) clearly shows uptake in stomach, kidneys, and left mediastinal metastasis known from CT (Fig. 15). Right scan shows ^{111}In-pentetreotide biodistribution in same patient 3 mo earlier (both scans at 24 h postinjection). Difference in size of metastatic lesion is due to tumor growth in 3-mo time interval between both scans.
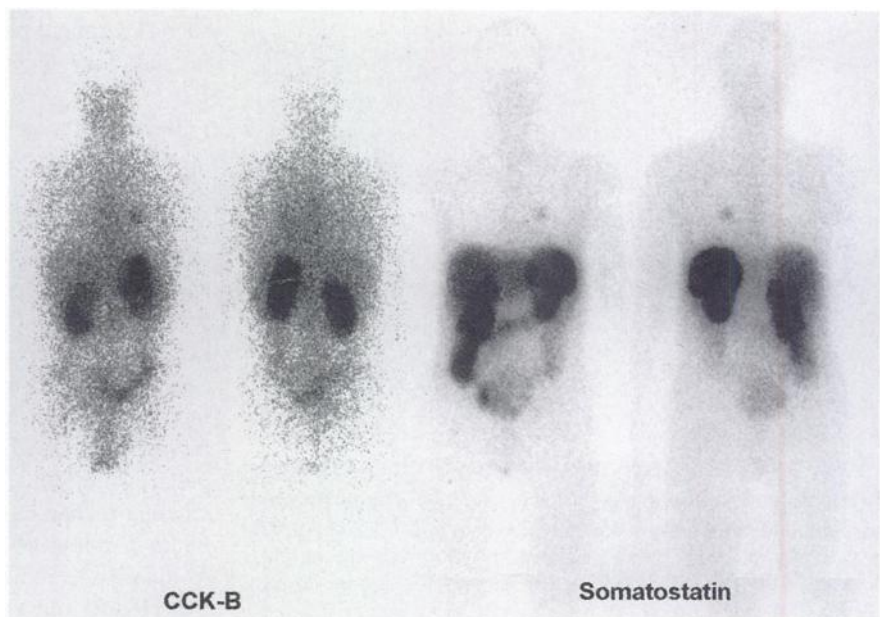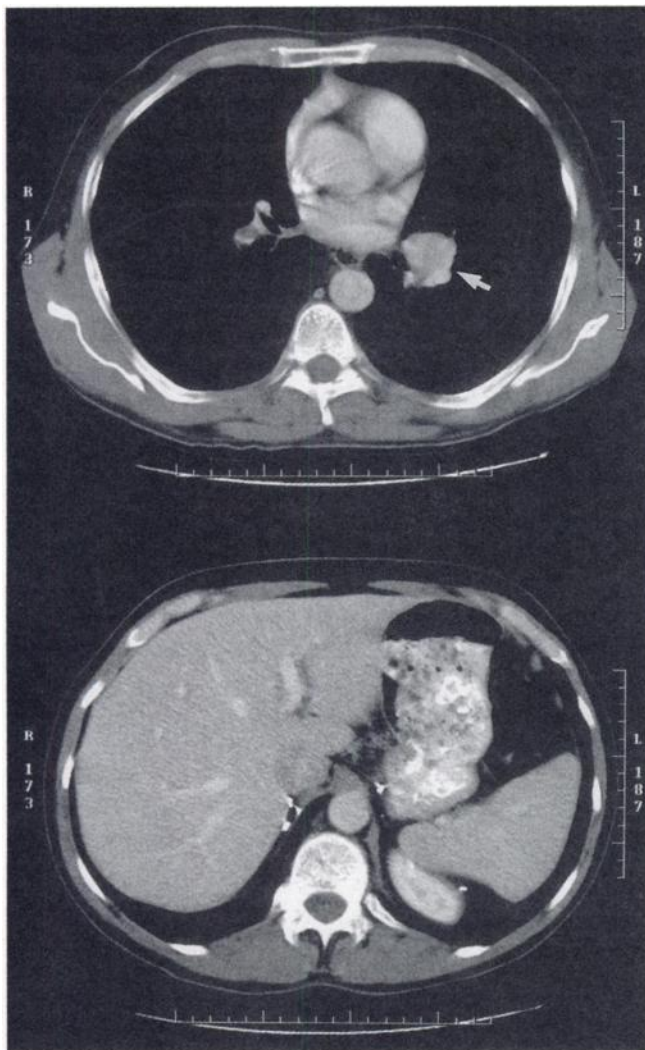
FIGURE 15. Chest CT of same patient as in Figure 14 shows 3-cm left hilar lymph node metastasis (arrow).

CCK-B receptor-binding peptides can improve the staging of MTC or small cell lung cancer in patients.

CONCLUSION

CCK/gastrin analogs may be a useful new class of receptor-binding peptides for diagnosis and therapy of CCK-B receptor-expressing tumors, such as MTC or small cell lung cancer, especially because there appears to be no dependence of the quantitative amount of receptor expression on the degree of tumor differentiation for CCK-B receptors (J.C. Reubi, oral communication, September 1998). This stands in clear contrast to somatostatin receptors, in which, in accordance with previous in vitro data (*39*), we were able to demonstrate in vivo the loss of somatostatin receptors in dedifferentiated and clinically more aggressive forms of MTC (*11*). Similar observations have been reported for the loss of somatostatin receptors in metastatic small cell lung cancer (*9,40*). Nonsulfated gastrin derivatives may be preferrable for scintigraphic purposes because of their CCK-B receptor selectivity, and hence lower accretion in

normal CCK-A receptor-expressing organs. The lack of physiological uptake in lymphatic tissues (e.g., the spleen) may be advantageous in the therapeutic application of CCK-B compared with somatostatin receptor ligands. Further preclinical and clinical studies are ongoing with radio-metal-labeled gastrin analogs.

REFERENCES

1. Reubi JC. Regulatory peptide receptors as molecular targets for cancer diagnosis and therapy. *Q J Nucl Med.* 1997;41:63–70.
2. Krenning EP, Kwekkeboom DJ, Pauwels S, Kvols LK, Reubi JC. Somatostatin receptor scintigraphy. In: Freeman LM, ed. *Nuclear Medicine Annual.* New York, NY: Raven Press; 1995:1–50.
3. Otte A, Mueller-Brand J, Dellas S, Nitzsche EU, Herrmann R, Maecke HR. Yttrium-90-labelled somatostatin-analogue for cancer treatment. *Lancet.* 1998;351: 417–418.
4. DeJong M, Breeman WA, Bernard BF, et al. Evaluation in vitro and in rats of ¹⁶¹Tb-DTPA-octreotide: a somatostatin analogue with potential for intraoperative scanning and radiotherapy. *Eur J Nucl Med.* 1995;22:608–616.
5. DeJong M, Bakker WH, Krenning EP, et al. Yttrium-90 and indium-111 labelling, receptor binding and biodistribution of [DOTA⁰,D-Phe¹,Tyr³]octreotide: a promising somatostatin analogue for radionuclide therapy. *Eur J Nucl Med.* 1997;24:368–371.
6. Virgolini I, Raderer M, Kurtaran A, et al. Vasoactive intestinal peptide-receptor imaging for the localization of intestinal adenocarcinomas and endocrine tumors. *N Engl J Med.* 1994;331:1116–1121.
7. van Hagen PM, Breeman WAP, Reubi JC, et al. Visualization of the thymus by substance P receptor scintigraphy in man. *Eur J Nucl Med.* 1996;23:1508–1513.
8. Safavy A, Khazaeli MB, Qin H, Buchsbaum DJ. Synthesis of bombesin analogues for radiolabeling with rhenium-188. *Cancer.* 1997;80:2354–2359.
9. Seregni E, Chiti A, Bombardieri E. Radionuclide imaging of neuroendocrine tumours: biological basis and diagnostic results. *Eur J Nucl Med.* 1998;25:639–658.
10. Behr TM, Gratz S, Markus PM, et al. Enhanced bilateral somatostatin receptor expression in mediastinal lymph nodes ("chimney sign") in occult metastatic medullary thyroid cancer: a typical site of tumor manifestation? *Eur J Nucl Med.* 1997;24:184–191.
11. Behr TM, Gratz S, Markus PM, et al. Anti-carcinoembryonic antigen antibodies versus somatostatin analogs in the detection of metastatic medullary thyroid carcinoma: are carcinoembryonic antigen and somatostatin receptor expression prognostic factors? *Cancer.* 1997;80:2436–2457.
12. Behr TM, Jenner N, Radetzky S, et al. Targeting of cholecystokinin-B/gastrin receptors in vivo: preclinical and initial clinical evaluation of the diagnostic and therapeutic potential of radiolabeled gastrin. *Eur J Nucl Med.* 1998;25:424–430.
13. Reubi JC, Waser B. Unexpected high incidence of cholecystokinin/gastrin receptors in human medullary thyroid carcinomas. *Int J Cancer.* 1996;67:644–647.
14. Reubi JC, Schaer JC, Waser B. Cholecystokinin (CCK)-A and CCK-B/gastrin receptors in human tumors. *Cancer Res.* 1997;57:1377–1386.

15. Smith JP, Stock EA, Wotring MG, McLaughlin PJ, Zagon IS. Characterization of the CCK-B/gastrin-like receptor in human colon cancer. *Am J Physiol.* 1996;271: R797–R805.

16. Mutt V. Historical perspectives on cholecystokinin research. *Ann N Y Acad Sci.* 1994;713:1–10.

17. Bolton AE, Hunter WM. The labelling of proteins to high specific radioactivities by conjugation to a 125I-containing acylating agent. *Biochem J.* 1973;133:529–539.

18. Hnatowich DJ, Layne WW, Childs RL, et al. Radioactive labeling of antibody: a simple and efficient method. *Science.* 1983;220:613–615.

19. Behr T, Fischer W, Peter-Katalinic J, Egge H. The structure of pneumococcal lipoteichoic acid: improved preparation, chemical and mass spectrometric studies. *Eur J Biochem.* 1992;207:1063–1075.

20. Behr T, Becker W, Hannappel E, Goldenberg DM, Wolf F. Targeting of liver metastases of colorectal cancer with IgG, F(ab')₂, and Fab' anti-CEA antibodies labeled with 99mTc: the role of metabolism and kinetics. *Cancer Res.* 1995;55:5777–5785.

21. Bacarese-Hamilton AJ, Adrian TE, Bloom SR. Prevention of cholecystokinin oxidation during tissue extraction. *Ann N Y Acad Sci.* 1985;448:571–572.

22. Zabel M, Grzeszkoviek F. Characterization of thyroid medullary carcinoma TT cell line. *Histol Histopathol.* 1997;12:283–289.

23. Behr TM, Wulst E, Radetzky S, et al. Improved treatment of medullary thyroid cancer in a nude mouse model by combined radioimmunochemotherapy: doxorubicin potentiates the therapeutic efficacy of radiolabeled antibodies in a radioresistant tumor type. *Cancer Res.* 1997;57:5309–5319.

24. Behr TM, Memtsoudis S, Sharkey RM, et al. Experimental studies on the role of antibody fragments in cancer radioimmunotherapy: influence of radiation dose and dose rate on toxicity and anti-tumor efficacy. *Int J Cancer.* 1998;77:787–795.

25. Rehfeld JF, Hansen HF, Marley PD, Stengaard-Pedersen K. Molecular forms of cholecystokinin in the brain and the relationship to neuronal gastrins. *Ann N Y Acad Sci.* 1985;448:11–23.

26. Reubi JC, Waser B, Läderach U, et al. Localization of cholecystokinin A and cholecystokinin B-gastrin receptors in the human stomach. *Gastroenterology.* 1997;112:1197–1205.

27. Ball DW, Baylin SB, de Bustros, AC. Medullary thyroid carcinoma. In: Braverman LE, Utiger RD, eds. *Werner and Ingbar's the Thyroid: A Fundamental and Clinical Text.* 7th ed. Philadelphia, PA: Lippincott/Raven Press; 1996:946–960.

28. Vanderhagen JJ, Crawley JN, eds. *Neuronal Cholecystokinin.* Vol. 448. New York, NY: New York Academy of Sciences; 1985.

29. Reeve Jr. JR, Eysselein V, Solomon TE, Go VLW, eds. *Cholecystokinin.* Vol. 713. New York, NY: New York Academy of Sciences; 1994.

30. Deschodt-Lanckman M. Enzymatic degradation of cholecystokinin in the central nervous system. *Ann N Y Acad Sci.* 1985;448:87–98.

31. Jakubke HD. *Peptide: Chemie und Biologie.* Heidelberg, Germany: Spektrum Akademischer Verlag; 1996.

32. Reeve JR, Eysselein VE, Ho FJ, et al. Natural and synthetic CCK-58: novel reagents for studying cholecystokinin physiology. *Ann N Y Acad Sci.* 1994;713:11–21.

33. Behr TM, Sharkey RM, Juweid ME, et al. Reduction of the renal uptake of radiolabeled monoclonal antibody fragments by cationic amino acids and their derivatives. *Cancer Res.* 1995;55:3825–3834.

34. Behr TM, Becker WS, Sharkey RM, et al. Reduction of the renal uptake of monoclonal antibody fragments by amino acid infusion. *J Nucl Med.* 1996;37:829–833.

35. Wank SA, Pisegna JR, DeWeerth A. Cholecystokinin receptor family: molecular cloning, structure, and functional expression in rat, guinea pig, and human. *Ann N Y Acad Sci.* 1994;713:49–66.

36. Reubi JC, Waser B, Schaer JC, et al. Unsulfated DTPA- and DOTA-CCK analogs as specific high-affinity ligands for CCK-B receptor-expressing human and rat tissues in vitro and in vivo. *Eur J Nucl Med.* 1998;25:481–490.

37. Nouel D, Faure M, St. Pierre J, Alonso R, Quirion R, Beaudet A. Differential binding profile and internalization process of neurotensin via neuronal and glial receptors. *J Neurosci.* 1997;17:1795–1803.

38. Duncan JR, Behr TM, DeNardo SJ. Intracellular fate of radiometals. *J Nucl Med.* 1997;38:829.

39. Reubi JC, Chayvialle JA, Franc B, Cohen R, Calmettes C, Modigliani E. Somatostatin receptors and somatostatin content in medullary thyroid carcinomas. *Lab Invest.* 1991;64:567–573.

40. Bohuslavizki KH, Brenner W, Günther M, et al. Somatostatin receptor scintigraphy in the staging of small cell lung cancer. *Nucl Med Commun.* 1996;17:191–196.